Available online at www.sciencedirect.com
SCIENCE DIRECT
Computer Vision and Image Understanding 102 (2006) 52–59
Computer Vision and Image Understanding
www.elsevier.com/locate/cviu

Automatic measurement of industrial sheetmetal parts with CAD data and non-metric image sequence

Yongjun Zhang *, Zuxun Zhang, Jianqing Zhang

School of Remote Sensing and Information Engineering, Wuhan University, Wuhan, 430079 Hubei, PR China

Received 26 August 2004; accepted 29 September 2005
Available online 9 November 2005

Abstract

A novel approach for three-dimensional (3D) reconstruction and measurement of industrial sheetmetal parts with computer aided design (CAD) data and non-metric image sequence is proposed. The purpose of our approach is to automatically reconstruct and measure the producing imprecision or deformations of industrial parts that are mainly composed of line segments, circles, connected arcs and lines. Principles of two-dimensional (2D) and one-dimensional (1D) least squares template matching to extract precise lines and points are presented. Hybrid point-line photogrammetry is adopted to obtain accurate wire frame model of industrial parts. Circles, arcs, and lines connected to each other on the part are reconstructed with direct object space solution according to known camera parameters. The reconstructed CAD model can be used for visual measurement. Experimental results of several parts are very satisfying. They show that the proposed approach has a promising potential in automatic 3D reconstruction and measurement of widely existed industrial parts mainly composed of lines, circles, connected arcs and lines.

Keywords: Photogrammetry; Industry; Part; CAD; Image sequence; Matching; Reconstruction; Measurement

1. Introduction

Three-dimensional (3D) reconstruction from imagery is one of the most active areas in close-range photogrammetry and computer vision. Nowadays, most industrial parts have their CAD data. The CAD models provide exact and complete description of the object geometries. Precision evaluation and quality control of parts with reference to corresponding CAD data receive attention in industrial communities. Reducing manpower, maintaining high precision and consistency and the time of measurement are the main foci of researchers.

Up to now, coordinate measurement machine (CMM) is the most widely used measuring equipment in industrial communities. The cost and speed of CMM are still major problems to be resolved [16]. Along with the development of computer vision, two-dimensional automated visual inspection has been widely used in Printed Circuit Board product lines [12]. A laser range sensor is used by [14] to digitize industrial parts into 3D point clouds, followed by registration of these 3D data with CAD model to inspect surface defects. Stereo vision technique with two CCD cameras and two LED lamps is used [11] in measurement of gaps on the automobile production line. Precision of about 0.1 mm within an planar area of 80 mm × 80 mm is obtained. Guha [7] presented a prototype of steel surface inspection system for identification of visual surface defects of Black Patch, Anneal Colour, Indentation Marks and Holes on cold rolled steel sheets. No quantitative description of the achieved precision has been addressed.

Although automated vision metrology is becoming more advanced (cf [5,1,13]), three-dimensional automatic inspection has been limited due to complexity of the problem [14]. Regarding the V-Stars system [6], precision of about 10–20 parts per million (ppm) can be achieved with one or more 2K × 3K cameras. However, special targets have to be

* Corresponding author. Fax: +86 27 68778086.
E-mail addresses: zhangyj@whu.edu.cn, yongjun_zhang@hotmail.com (Y. Zhang).

1077-3142/$ - see front matter © 2005 Elsevier Inc. All rights reserved.
doi:10.1016/j.cviu.2005.09.002

attached onto the surface of the interested object, which makes the system less efficient. Furthermore, there is no practical 3D vision system that can substitute man's efforts in imprecision measurement and quality control for widely existed sheetmetal parts.

Line photogrammetry is widely used in reconstruction of objects mainly represented by polyhedral models [3,9,10]. Photogrammetric techniques are also used in reconstruction of industrial installations [18] and reverse engineering [4] with CAD models. Although all of these systems are semi-automatic and time-consuming, line photogrammetry still exhibits potential in automatic 3D reconstruction, especially in the case of known initial models of the interested objects.

A new approach in reconstructing and measuring industrial sheetmetal parts with CAD data and non-metric image sequence is proposed in this paper. The general purpose is to reconstruct and measure industrial parts quickly and accurately with hybrid point-line photogrammetry and direct object space solution through CAD data and information extracted from the imagery. A planar grid is used to calibrate the non-metric CCD camera and provide initial values of camera parameters during reconstruction. World coordinate system chosen is the same as that of the grid. CAD data represents the initial model and the topology of the reconstructed part. Least-squares template matching (LSTM) and several matching results are discussed in Section 2. Afterwards, detailed approaches of how to reconstruct industrial parts are presented. The reconstructed CAD model can be used to measure the producing imprecision or deformations of the part. Section 4 discusses the experimental results. Conclusions and future work are outlined in Section 5.

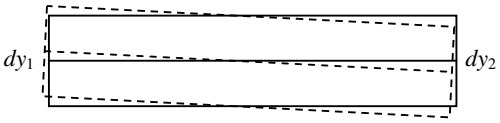

Fig. 1. Two unknowns in line template matching.

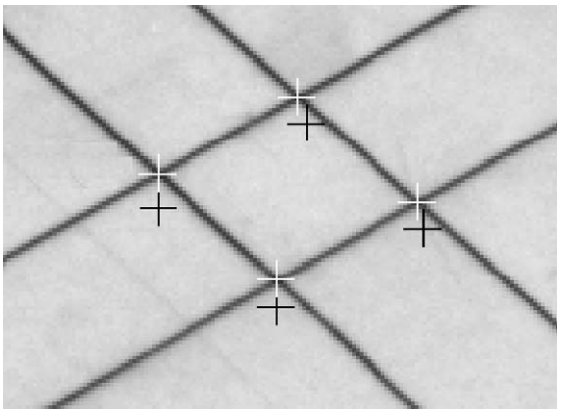

Fig. 2. Initial projections and matched results of points.

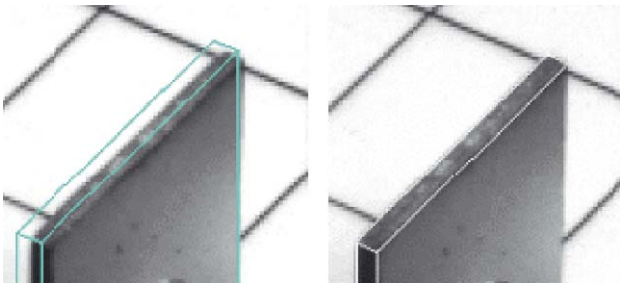

Fig. 3. Initial projections and matched results of lines.

2. Least squares template matching

2.1. Two-dimensional line template matching

Image points and lines are the most effective features that are used for 3D reconstruction of objects in photogrammetry and computer vision communities. If "Minimization of the squared sum of grey-difference" is chosen as criteria, the image matching equation can be written as $\sum vv = \min$. If only random noises are considered, the error equation of image matching will be $v = g_1(x,y) - g_2(x,y)$, where v is the difference between two grey values g_1 and g_2 of two image blocks, respectively. This is the basic principle of least-squares template matching [15] which is widely used in digital photogrammetry. Line template matching is a 2D matching technique that attempts to match a standard image block (so called template) with a real image patch. The length of the image window is usually longer than 10 pixels. The real image patch is usually rotated horizontal to facilitate the matching process. As shown in Fig. 1, the level rectangle represents the standard template, while the dashed rectangle is the image patch to be matched. Displacement along the center line is not important in image matching. However, the angle between template and image must be eliminated. Two unknowns dy_1 and dy_2 are essential to fit the small rotation angles between the template and the image patch.

The line template matching technique can be used for extracting of image line features precisely. Grid points can be detected by the intersection of two matched lines of each corner, as shown in Fig. 2. The black crosses are the predicted image corners. And the white crosses are the matched ones. The precision of image matching results is higher than 0.05 pixels.

Left of Fig. 3 shows the initial projections of line segments of the part. The initial image lines are usually several pixels from the real image features. Although rust exists on the part, the matched image lines are well fitted to the real image features (right of Fig. 3). Actually, the matching precision is also higher than 0.05 pixels.

2.2. One-dimensional point template matching

As we know, a line can be represented by a group of small colinear segments. If the image window of line

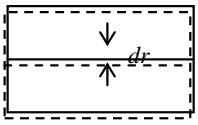

Fig. 4. One unknown in point template matching.

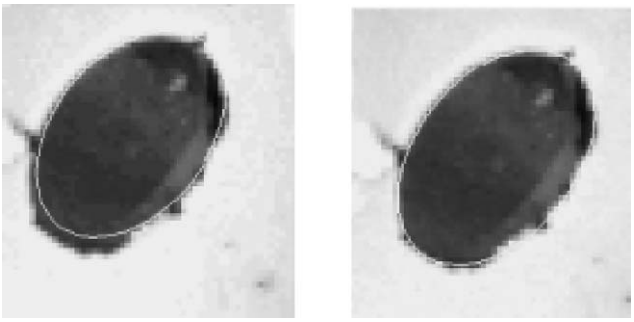

Fig. 5. Initial projection and matched result of a circle.

template matching is subdivided into small segments, each with a length of 2–5 pixels named "point segment," the rotation angles between standard templates and small point segments can be neglected. Matching between the "point segment" and the standard template is called point template matching in this paper. As it differs from line template matching, there is only one unknown dr for 1D point template matching, as shown in Fig. 4. Fig. 5 shows the initial projection and matched result of a circle by 1D point template matching. Although rust is evident, the matched circle is well fitted to the image, showing the potential of 1D point template matching.

3. Reconstruction of industrial parts

The topology of sheetmetal part presented by CAD data is assumed to be correct since it is designed on computer and often checked before the part is produced. The geometry of the real part is usually not identical to the CAD data due to mis-operation during production or deformations after a period of usage. It is important for quality control to know whether the real part and the designed one are identical. Approaches detailing of how to reconstruct correct geometric model with designed data and information extracted from imagery will be discussed.

3.1. Reconstruction of wire frame model

The origin of the grid coordinate system is located at the centre of the planar grid, X and Y-axes in the grid plane and Z-axis upright. World coordinate system is chosen the same as that of the grid. Generally speaking, the coordinate system of the industrial part defined in CAD data is not identical with the world coordinate system. There are six elements (rotation + translation) to convert the CAD coordinate system into world coordinate system.

Sheetmetal parts are mostly composed of line segments. This is the reason that we choose line photogrammetry to reconstruct and measure them. As shown in Fig. 6, the image line pq, space line PQ and the projection center S should be coplanar, while p and P, q, and Q are not necessarily correspondences, which is the most important advantage of line photogrammetry [3]. A line in the image can be parameterised in several ways. Two end points are used here, because it is singularity-free and easy to setup error equations.

The coplanar equation among p, S, P, and Q is

$$\begin{vmatrix} u_p & v_p & w_p \\ X_P - X_S & Y_P - Y_S & Z_P - Z_S \\ X_Q - X_S & Y_Q - Y_S & Z_Q - Z_S \end{vmatrix} = 0, \tag{1}$$

where (u_p, v_p, w_p) is the model coordinate of image point p, (X_S, Y_S, Z_S) the coordinate of camer center S, (X_P, Y_P, Z_P) and (X_Q, Y_Q, Z_Q) the coordinates of part points P and Q. The error equation of line photogrammetry can be written as

$$\begin{aligned} &A_1 \mathrm{d}x_p + A_2 \mathrm{d}y_p + A_3 \mathrm{d}\varphi + A_4 \mathrm{d}\omega + A_5 \mathrm{d}\kappa + A_6 \mathrm{d}X_S \\ &\quad + A_7 \mathrm{d}Y_S + A_8 \mathrm{d}Z_S + A_9 \mathrm{d}\varphi^0 + A_{10} \mathrm{d}\omega^0 + A_{11} \mathrm{d}\kappa^0 \\ &\quad + A_{12} \mathrm{d}\Delta X^0 + A_{13} \mathrm{d}\Delta Y^0 + A_{14} \mathrm{d}\Delta Z^0 + A_{15} \mathrm{d}X_P^0 \\ &\quad + A_{16} \mathrm{d}Y_P^0 + A_{17} \mathrm{d}Z_P^0 + A_{18} \mathrm{d}X_Q^0 + A_{19} \mathrm{d}Y_Q^0 + A_{20} \mathrm{d}Z_Q^0 \\ &\quad + F_X = 0, \end{aligned} \tag{2}$$

where A_1–A_{20} are the partial derivatives of unknowns and F_X the constant item, dx_p, dy_p the corrections of end point p, dφ, dω, dκ, dX_S, dY_S, dZ_S the corrections of camera parameters, $\mathrm{d}\varphi^0, \mathrm{d}\omega^0, \mathrm{d}\kappa^0, \mathrm{d}X_S^0, \mathrm{d}Y_S^0, \mathrm{d}Z_S^0$ the corrections of six parameters (rotation and translation) between the part and the world coordinate system, $\mathrm{d}X_P^0, \mathrm{d}Y_P^0, \mathrm{d}Z_P^0$ and $\mathrm{d}X_Q^0, \mathrm{d}Y_Q^0, \mathrm{d}Z_Q^0$ the corrections of part points P and Q.

Besides the coplanar equation among p, S, P, and Q, there exits another equation among q, S, P, and Q. The linearized form is similar to that of Eq. (2).

For parts that are very simple or for those that are a few line segments, the geometric configuration is very poor.

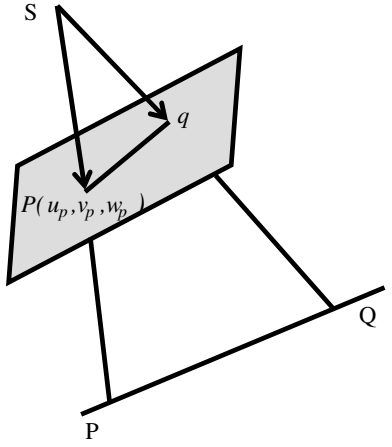

Fig. 6. Coplanarity between space and image lines.

Grid points should be combined into the adjustment model to ensure the reliability of reconstruction. Error equations of grid points are:

$$\begin{aligned} v_x &= B_1 \mathrm{d}\varphi + B_2 \mathrm{d}\omega + B_3 \mathrm{d}\kappa + B_4 \mathrm{d}X_S + B_5 \mathrm{d}Y_S \\ &\quad + B_6 \mathrm{d}Z_S + B_7 \mathrm{d}X + B_8 \mathrm{d}Y + B_9 \mathrm{d}Z - l_x, \\ v_y &= C_1 \mathrm{d}\varphi + C_2 \mathrm{d}\omega + C_3 \mathrm{d}\kappa + C_4 \mathrm{d}X_S + C_5 \mathrm{d}Y_S \\ &\quad + C_6 \mathrm{d}Z_S + C_7 \mathrm{d}X + C_8 \mathrm{d}Y + C_9 \mathrm{d}Z - l_y, \end{aligned} \tag{3}$$

where l_x, l_y are constant items; $B_1, \ldots, B_9$, $C_1, \ldots, C_9$ coefficients of unknowns; $\mathrm{d}X$, $\mathrm{d}Y$, $\mathrm{d}Z$ the corrections of grid points; and $\mathrm{d}\varphi$, $\mathrm{d}\omega$, $\mathrm{d}\kappa$, $\mathrm{d}X_S$, $\mathrm{d}Y_S$, $\mathrm{d}Z_S$ the corrections of camera parameters. Please refer to [15] for more detail about the coefficients of error equations. If the coordinates of grid points can be treated as known, terms of $\mathrm{d}X$, $\mathrm{d}Y$, $\mathrm{d}Z$ should be removed from the error equations. The model of hybrid point-line photogrammetry is composed of Eqs. (2) and (3). It can be used to reconstruct the wire frame model of parts.

3.2. Reconstruction of complex shapes

For lots of board-like (sheetmetal) industrial parts, the reconstruction of complex shapes is also very important but hard to deal with in practice. An effective approach to reconstruct circles, connected arcs and lines based on 1D point template matching and direct object space solution will be presented.

Camera parameters, which can be obtained with hybrid point-line photogrammetry in Section 3.1, can be treated as known in the process of reconstructing complex shapes. The end points of small line segments are the result of template matching and also functions of space circles or lines. The parameters of space circles or lines and their image features are related by mathematical models. Thus parameters of circles, arcs, and lines can be obtained directly from several images by least squares template matching.

To facilitate the reconstruction process, suppose the plane where the circle or arc lies in is known. This is true since the plane can be determined with the reconstructed wire frame model of the part. The camera parameters of the images can be rotated to generate a level plane. So the circle equation in the level plane is very simple:

$$\begin{aligned} X &= X_0 + R \cdot \cos\theta, \\ Y &= Y_0 + R \cdot \sin\theta, \end{aligned} \tag{4}$$

where X_0, Y_0 and R are the center and radius of circle or arc. θ varies from 0 to 360 degree for circle, and from start angle to end angle for arc. In this paper, circles and arcs are represented by a number of points with certain intervals of different angle θ. The top of Fig. 7 is a space circle, and the bottom is the projected ellipse with known camera parameters. Each point A on the space circle defined by θ has its corresponding point a in the image.

If Eq. (4) is combined into collinearity equations, the unknowns are the center and radius of circle or arc. For certain angle θ, the object point is projected onto the image

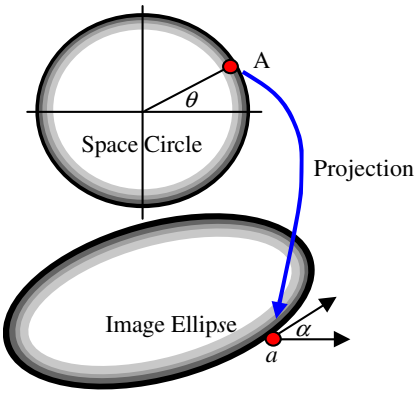

Fig. 7. Projected image point of circle.

and the tangential vector with angle α can be easily determined. A small window (with 2–5 pixels length) taken the projected image point as center and α as tangential vector is rotated into horizontal, followed by 1D template matching. The displacement $\mathrm{d}r$ determined by template matching can be rotated back to the original image coordinate system according to α. Error equations of circle or arc reconstruction can be written as:

$$\begin{aligned} v_x &= A_1 \cdot \mathrm{d}X_0 + A_2 \cdot \mathrm{d}Y_0 + A_3 \cdot \mathrm{d}R - \mathrm{d}x, \\ v_y &= B_1 \cdot \mathrm{d}X_0 + B_2 \cdot \mathrm{d}Y_0 + B_3 \cdot \mathrm{d}R - \mathrm{d}y, \end{aligned} \tag{5}$$

where A_1, A_2, A_3, B_1, B_2, B_3 are the coefficients of unknowns, $\mathrm{d}x$, $\mathrm{d}y$ constant items, X_0, Y_0, and R are the center and radius, respectively. Thus, the parameters of space circles or arcs can be obtained directly from one or several images by LSTM with initial values obtained from CAD data. The obtained parameters of circles or arcs should be rotated back to the world coordinate system to get the reconstructed model.

Arcs in parts are usually connected to lines. As shown in Fig. 8, two arcs c_1, c_2 and three line segments l_1, l_2, and l_3 are connected to each other. Generally, they are very difficult to reconstruct precisely. The model of obtaining optimum solution of arcs and lines will be addressed. For convenience of reconstruction, line segments are also rotated into a level plane, and represented as follows:

$$\begin{aligned} X &= X_t + \mathrm{i} \cdot \Delta L \cdot \cos\beta, \\ Y &= Y_t + \mathrm{i} \cdot \Delta L \cdot \sin\beta, \end{aligned} \tag{6}$$

where X_t, Y_t is the start point of line segment, β is the direction of the line, ΔL is the length of small segment

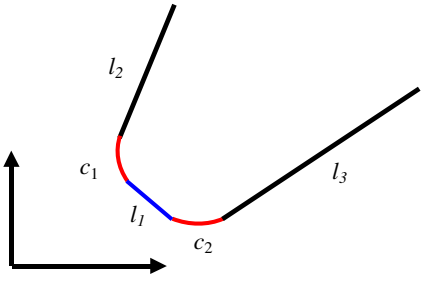

Fig. 8. Connected arcs and lines.

approximately equal to the length of point window in the circle and arc reconstruction. Error equations of line reconstruction are:

$$\begin{aligned} v_x &= M_1 \cdot \mathrm{d}X_t + M_2 \cdot \mathrm{d}Y_t + M_3 \cdot \mathrm{d}\beta - \mathrm{d}x, \\ v_y &= N_1 \cdot \mathrm{d}X_t + N_2 \cdot \mathrm{d}Y_t + N_3 \cdot \mathrm{d}\beta - \mathrm{d}y, \end{aligned} \tag{7}$$

where M_1, M_2, M_3 and N_1, N_2, N_3 are coefficients of unknowns, $\mathrm{d}x$, $\mathrm{d}y$ constant items, $\mathrm{d}X_t$, $\mathrm{d}Y_t$ and $\mathrm{d}\beta$ are the corrections of the start point and direction of the line segment. The circle or arc reconstruction Eq. (5) can be combined with line reconstruction Eq. (7) to get an uniform solution of connected arcs and lines. To ensure the stability of reconstruction, geometric constrains should be added, such as the center of arc c_1 should lies on the bisector of line l_1 and l_2; the center of arc c_2 which should lie on the bisector of line l_1 and l_3 and three lines which should be tangential to the two arcs, etc.

4. Experiments

4.1. Overview of the system

To reduce the cost of the system, only one non-metric CCD camera with 1300 pixels × 1030 pixels resolution is used. Fig. 9 shows the hardware configuration of the system. A planar grid is fixed on the rotation table for camera calibration and offering initial values of camera parameters for reconstruction. As mentioned in Section 3, the world coordinate system is chosen to be the same as that of the grid. The part to be reconstructed is put approximately on the center of the grid. To facilitate the determination of 3D rigid transformation parameters (rotation and translation) between the part and the world coordinate system, the distance between two origins of the two coordinate systems need to be shorter than 10 mm, and the angles between axes of the two coordinate systems should be smaller than 10°. To generate diffused illumination for the grid and the part, four home-used lamps are encapsulated in a semi-transparent plastic box. Image sequence is obtained while the table rotates against its rotating axis under computer control.

Fig. 9. Hardware configuration of the measurement system.

The developed software runs fully automatically. It can be used to reconstruct and measure industrial parts mainly composed of lines, circles, connected arcs and lines. The system is composed of four steps. First, image sequence is acquired by CCD digital camera automatically while the table turns around its center controlled by computer. Image points and lines are obtained by LSTM simultaneously with image acquiring. Then 3D wire frame model of the part is reconstructed with hybrid point-line photogrammetry. Afterwards, circles, connected arcs and lines are reconstructed by direct object space solution. Finally, measurements can be done automatically or interactively.

4.2. Real data experiments

The measurement system has been tested with real image data of many sheetmetal parts taken by a pre-calibrated CCD camera [19]. Experiments of two parts both with the dimension of about 150 mm will be presented in the following. The part to be reconstructed is put on the center of the planar grid, which is fixed on the turntable. The CCD camera is fixed on a tripod with a distance of about 600 mm to the part. One image of each part is shown in Fig. 10. To get a general idea of how many images are needed for 3D reconstruction, a sequence with 50 images for part one is taken with equal angle intervals, while 25 images is taken for part two. Image matching is made simultaneously with image acquiring. Grid points are detected as the intersection of two line segments fitted to each corner. Lines are obtained by LSTM with initial values projected by the CAD data and the camera parameters

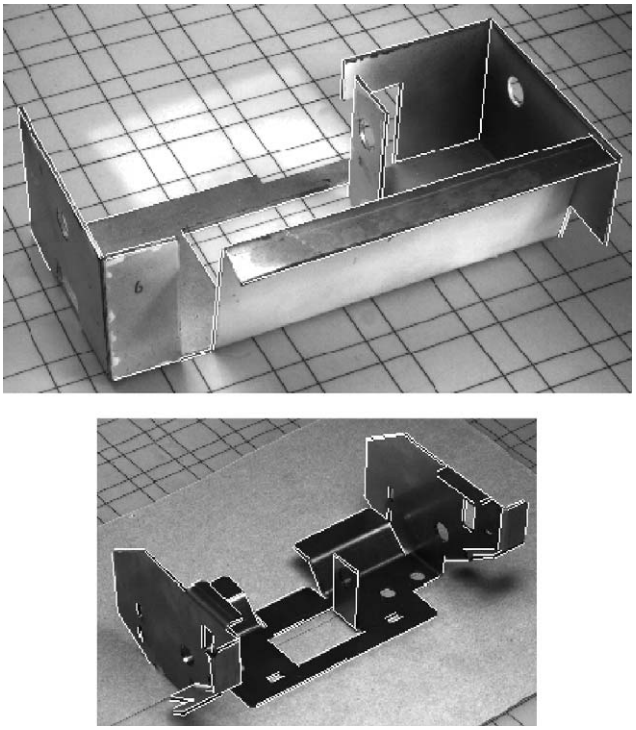

Fig. 10. One image for each part to be measured.

provided by the grid. There are inevitably many occlusions during line template matching since the industrial part is three-dimensional. Fortunately, the initial model of the part and the camera parameters of each image are known. So while the initial model is projected onto the image, visible and invisible lines can be determined by occlusion analysis, which is well-known in Computer Graphics [2]. For lines that are not visible in the image are removed before image matching to avoid mismatches.

White lines in Fig. 10 are the matched lines of parts. There is nearly no mismatch for points of the grid. But for parts that are very thin or with shadows in the nearby, there maybe some mismatched lines. Most of them can be successfully removed with Trifocal Tensor [8] computed with known camera parameters. The remained mismatches can be eliminated by the followed iterative least squares bundle adjustment during reconstruction by blunder (outlier) detection techniques that are very popular in Photogrammetry and Computer Vision [15,17].

The system can generate a final CAD model for each industrial part within 3 min (including the image acquiring) in a PIV personal computer. To evaluate the relationship between the image number involved and the precision of reconstruction, 50 images and 25 images (every two of the 50 images) are used to reconstruct part one, while all the 25 images are used to reconstruct part two. Reconstructed models of the two parts are displayed with OpenGL, Fig. 11A is the 3D model of part one reconstructed with 50 images. Fig. 11B is the 3D model of part two reconstructed with 25 images. These 3D models can be used to measure the producing imprecision (or deformation) either automatically or interactively.

To evaluate the precision of the reconstruction and measurement system, 25 distances between lines and planes of part one are measured by callipers and compared with that computed by the reconstructed CAD model. The distance between a line and a plane is defined as the mean of two distances from the two end points of a line to the plane determined by all points in it. Coordinates of all points are obtained from the reconstructed CAD model. Distances between lines, and planes are defined in a similar way. "Producing imprecision" means distances between lines, planes or line to plane measured by callipers subtracting the corresponding distances obtained from the CAD data. "Computed imprecision" means distances computed with the reconstructed CAD model subtracting the corresponding designed distances.

Figs. 12A and 12B show the measuring results of part one reconstructed with 50 and 25 images, respectively. It is very clear that the two measuring results are nearly identical. It can also be seen from Fig. 12 that the largest "producing imprecision" of the part is about 0.5 mm, i.e., the maximum difference between the real part and the designed CAD model is 0.5 mm. Note that all imprecision larger than 0.1 mm can be accurately detected by the proposed system. The RMS error of deviations between the measured and computed distances is both 0.069 mm for part

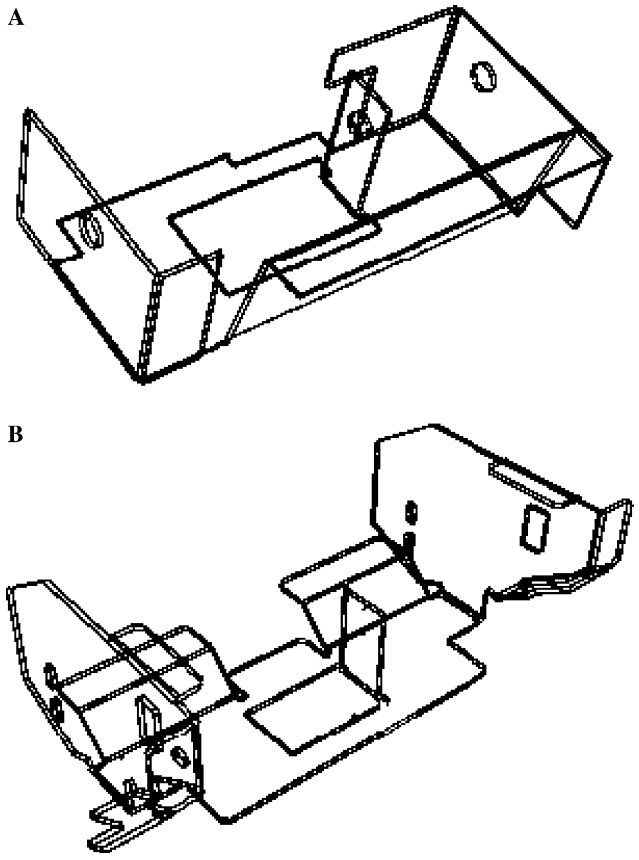

Fig. 11. Reconstructed 3D view of the two parts.

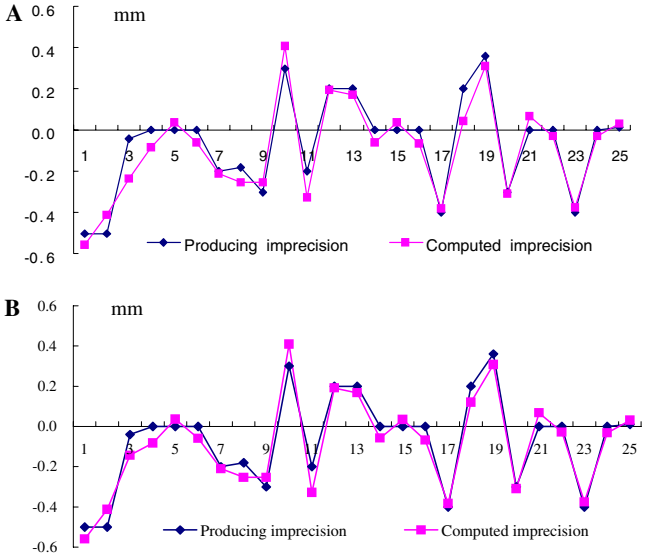

Fig. 12. Measuring results of part one with 50(A) and 25(B) images.

one either with 50 or 25 images. It means that 25 images are enough to reconstruct this kind of sheetmetal parts. This is the reason that only 25 images are taken for part two.

Measuring results with 25 distances of part two is shown in Fig. 13. Measured distances of part two are very close to

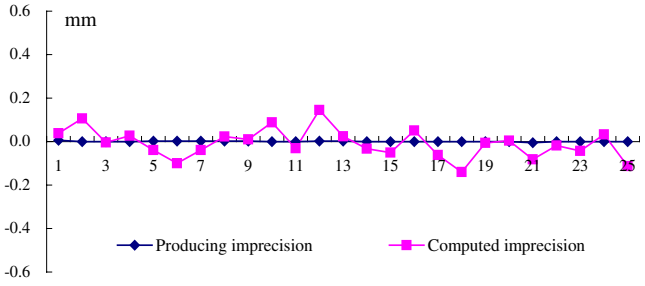

Fig. 13. Measuring results of part two.

that of the CAD data, i.e., the producing imprecision is nearly zero. Deviation of computed imprecision shows a well normal distribution. RMS error of deviation is 0.067 mm for the part.

The relative precision, which can be calculated as the ratio of RMS against the distance between the camera and the part, are both higher than 1/8500 (0.069 mm/600 mm = 1/8700) for the two parts, which shows the precision of the proposed system when manually measured distances are treated as errorless. Actually, distances measured by callipers cannot be errorless. The precision of callipers is usually 0.02 mm. From the law of covariance propagation [15,17], we have $\sqrt{0.069^2 - 0.02^2} = 0.0687$. So precision of the proposed system should be higher than 1/8000.

Other three sheetmetal parts with dimension of about 102, 98, and 100 mm have also been used for experiments. Experimental configurations are exactly the same as the two parts already discussed. Three designed distances between two planes of the three parts (one distance for each part) are all 100 mm, as listed in the first column of Table 1. The measured distances by our system are shown in the second column. Actually, as shown in the third column, the real distances are approximately 102, 98, and 100 mm, respectively. As can be seen from the fourth column, although the producing imprecision are nearly 2 mm, the maximum difference between the measured and computed distances is about 0.06 mm.

Three designed angles between two planes of the three parts (one angle for each part) are all 90° (first column of Table 2), while actually they are about 92°, 88°, and 90°, respectively (third column). When compared with the measured angles shown in the second column, differences are well below 0.1°.

The proposed circle reconstruction approach is also tested with several real image data. Fig. 14A shows two projections of a circle with CAD data and camera parameters obtained from hybrid point-line photogrammetry. As can be seen, there are many rusts on the circle. The reconstructed projections (Fig. 14B) are well fitted with actual image ones. The diameter of reconstructed circle is 9.948 mm, very close to the real value 10.00 mm measured by callipers.

Table 1
Results of distances of the three parts (mm)

Designed	Measured	True	Difference
100.000	101.8704	101.8083	0.0621
100.000	97.9202	97.8733	0.0469
100.000	99.9311	99.9867	−0.0556

Table 2
Results of angles of the three parts (degree)

Designed	Measured	True	Difference
90.000	88.1491	88.2044	−0.0553
90.000	92.0371	91.9765	−0.0605
90.000	89.6530	89.6733	−0.0203

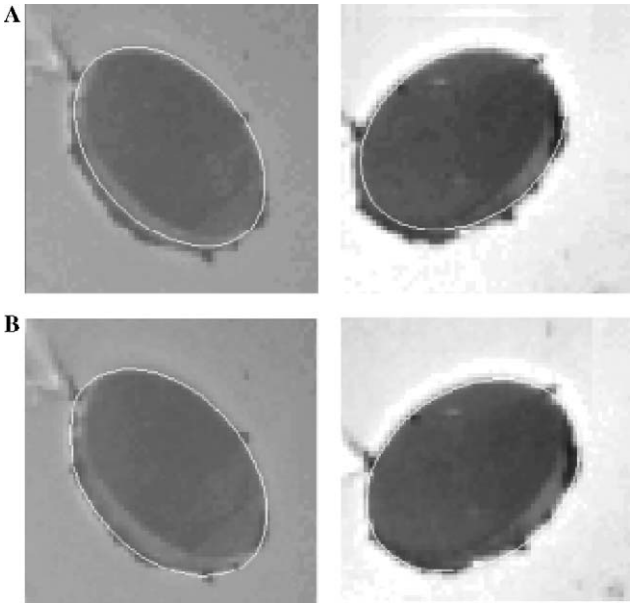

Fig. 14. Initial (A) and reconstructed; (B) projections of a circle.

Fig. 15A shows the initial projections in 2 images of 4 arcs and 4 lines connected to each other. The length of the shorter line segments is only about 12 pixels in the image, and even a few pixels for the arcs. It is very difficult to reconstruct with common strategies because it is very small in the image. But for the proposed technique of object space solution with geometric constraints, they can be reconstructed successfully and stably. High precision image matching technique and geometric constraint among components is the biggest contribution to reconstruct this kind of entities. The projection of reconstructed model is also well fitted to images (Fig. 15B).

As can be seen, the precision of our system is higher than that of [11], which can achieve a precision of 0.1 mm within an planar area of 80 mm × 80 mm. What most important is that our system can generate 3D model of industrial parts without attaching any marks. The hardware configuration is also cheaper. Furthermore, there are seldom publications or systems that can reconstruct circles, connected arcs and lines without attaching any marks on the surface.

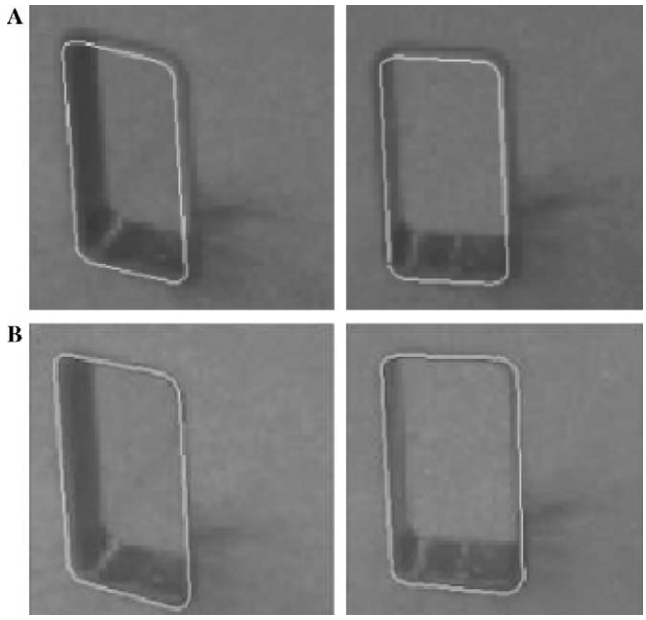

Fig. 15. Initial (A) and reconstructed; (B) projections of connected arcs and lines.

5. Conclusions

An effective approach for 3D reconstruction and measurement of industrial parts mainly composed of line segments, circles, connected arcs and lines with non-metric image sequence and CAD data is proposed. The wire frame model can be accurately reconstructed with hybrid point-line photogrammetry. Circles, arcs, and lines connected to each other are successfully reconstructed by 1D point template matching and direct object solution with known camera parameters from hybrid adjustment.

Experiments of real images are very satisfying. The relative precision is higher than 1/8000, and all imprecision larger than 0.1 mm can be detected accurately. The proposed technique of reconstruction and measurement also has the advantages of low cost of hardware and fully automatic. It is promising in automatic 3D reconstruction and measurement of industrial parts mainly composed of lines, circles, connected arcs and lines.

However, the proposed system still requires further improvements. Relation between illumination condition and precision of measurement has to be analysed. More investigations will be done to obtain best image number for sheetmetal parts with different complexity. The contribution of one more cameras integrated into the proposed system besides the camera already used also need to be performed in the near future.

Acknowledgments

This work is partly supported by National Natural Science Foundation of China (NSFC) with Project Nos. 40301041 and 40371099.

References

[1] M. Chang, C. Fuh, Fast search algorithms for industrial inspection, Int. J. Pattern Recogn. Artif. Intell. 15 (4) (2001) 675–690.
[2] D. Cohen-Or, Y. Chrysanthou, C. Silva, F. Durand, A Survey of visibility for walkthrough applications, IEEE Trans. Visual. Comput. Graph. 9 (3) (2003) 412–431.
[3] P. Debevec, Modelling and Rendering Architecture from Photographs: A hybrid Geometry- and Image-based Approach, University of California at Berkeley, 1996.
[4] P. Ermes, Constrains in CAD Models for Reverse Engineering using Photogrammetry, IAPRS 33 (B5/1) (2000) 215–221.
[5] C. Fraser C., Automated vision metrology: a mature technology for industrial inspection and engineering surveys, in: 6th South East Asian Surveyors Congress, Western Australia, 1999.
[6] GSI, 2003. V-STARS Main Brochure. Geodetic Services Inc. http://www.geodetic.com/vstars.htm.
[7] P. Guha, Automated Visual Inspection of Steel Surface Texture Segmentation and Indian Institute Of Technology, Indian Institute Of Technology, Kanpur India, 2001.
[8] R. Hartley, A. Zisserman, Multiple View Geometry in Computer Vision, Cambridge University Press, UK, 2000.
[9] F.A. van den Heuvel, A Line-photogrammetry mathematical model for the reconstruction of polyhedral objects, Proc. SPIE 3641 (1999) 60–71.
[10] F.A. van den Heuvel, Automation in Architectural Photogrammetry, Line Photogrammetry for the Reconstruction from Single and Multiple Images. PhD Thesis, Technical University of Delft, 2003.
[11] D. Kosmopoulos, T. Varvarigou, Automated inspection of gaps on the automobile production line through stereo vision and specular reflection, Comput. Indus. 46 (2001) 49–63.
[12] M. Moganti, F. Ercal, C.H. Dagli, et al., Automatic PCB inspection algorithms: a survey, Comput. Vis. Image Understand. 63 (2) (1996) 287–313.
[13] R. Pappa, T. Jones, J. Black, et al., Photogrammetry Methodology Development for Gossamer Spacecraft Structures, NASA/TM-2002-211739. Langley Research Center, USA, 2002.
[14] F. Prieto, P. Boulanger, H.T. Redarce, et al., Visual System for Fast and Automated Inspection of 3D Parts, Int. J. CAD/CAM Comput. Graph. 13 (4) (1998) 211–227.
[15] T. Schenk, Digital Photogrammetry, Vol. I. TerraScience, USA, 1999.
[16] S. Steven, Dimensional Inspection Planning for Coordinate Measuring Machines. PhD Thesis, University of Southern California, 1999.
[17] B. Triggs, P. McLauchlan, R. Hartley, A. Fitzgibbon, Bundle adjustment—a modern synthesis. proceedings of the international workshop on vision algorithms: theory and practice, LNCS 1883 (1999) 298–372.
[18] G. Vosselman, J.W.H. Tangelder, 3D Reconstruction of Industrial Installations by Constrained Fitting of CAD models to images, in: G. Sommer (Ed.), Mustererkennung 2000, Springer, Berlin, 2000, pp. 285–292.
[19] Y. Zhang, Z. Zhang, J. Zhang, Camera calibration technique with planar scenes, Proc. SPIE 5011 (2003) 291–296.